

# Low Complexity ICI Mitigation for MIMO-OFDM in Time-Varying Channels

Jinxing Hao, Jintao Wang, and Changyong Pan

**Abstract**—Time-varying channels destroy the orthogonality among subcarriers in orthogonal frequency division multiplexing (OFDM) systems, and introduce intercarrier interference (ICI). Lots of efforts have been devoted to mitigate ICI in OFDM systems, with different frame structures and channel models, but the computational complexity of the methods is usually very high. In multiple-input multiple-output (MIMO) systems, the complexity is even higher. In this paper, a low-complexity ICI mitigation method is proposed for MIMO-OFDM systems under the assumption of linear time-varying channels. It reduces the complexity of ICI compensation from  $O(K^3(N^3 + MN^2 + MN) + NK \log(K))$  to  $O(K(N^3 + 2MN^2 + 2MN + 2M^2 + N \log(K)))$ , where  $K$  is the number of subcarriers,  $M$  the number of transmitters, and  $N$  the number of receivers. It requires channel estimation based on the linear time-varying channel model, and no transmission overhead is needed. The proposed algorithm applies to all OFDM systems as long as linear time-varying channel estimation is applicable. Time-domain synchronous-OFDM naturally suits for the proposed ICI mitigation algorithm because its receiver is able to easily estimate linear time-varying channels. Simulation with QPSK and 16QAM modulation demonstrates the performance of the proposed method, in comparison with no ICI mitigation case. It shows that 2 dB signal to noise gain is achieved when the uncoded bit error rate is  $10^{-3}$  and the normalized Doppler frequency is 0.1.

**Index Terms**—Multiple-input multiple-output orthogonal frequency division multiplexing (MIMO-OFDM), inter-carrier interference (ICI) mitigation, time domain synchronous orthogonal frequency-division multiplexing (TDS-OFDM), low complexity.

Manuscript received January 6, 2016; revised March 7, 2016; accepted March 8, 2016. This work was supported in part by the Beijing Higher Education Young Elite Teacher Project under Grant YETP0101, in part by the National Science Foundation of China under Grant 61471221, in part by the Science and Technology Partnership Program through the Ministry of Science and Technology of China, and in part by the AQSIQ Project of Standardization Administration of People's Republic of China under Grant DTV-001.

J. Hao and J. Wang are with the Department of Electronic Engineering, Tsinghua University, Beijing 100084, China, also with the Tsinghua National Laboratory for Information Science and Technology, Tsinghua University, Beijing 100084, China, and also with the Shenzhen City Key Laboratory of Digital TV System, Shenzhen 518057, China (e-mail: haojx11@mails.tsinghua.edu.cn; wangjintao@tsinghua.edu.cn).

C. Pan is with the Tsinghua National Laboratory for Information Science and Technology, Tsinghua University, Beijing 100084, China, and also with the Shenzhen City Key Laboratory of Digital TV System, Shenzhen 518057, China (e-mail: pcy@tsinghua.edu.cn).

Color versions of one or more of the figures in this paper are available online at <http://ieeexplore.ieee.org>.

Digital Object Identifier 10.1109/TBC.2016.2550763

## I. INTRODUCTION

ORTHOGONAL frequency division multiplexing (OFDM) has been successfully applied in vast areas of broadband communications [1]–[3]. Conventionally, OFDM systems assume the channel remains static in one OFDM symbol duration, thus one-tap equalizer would be sufficient for equalization on a specific subcarrier. However, this assumption may not always be effective in high-speed mobile environment, such as in the broadcasting channels, in the cellular uplink/downlink channels on high-speed railway or in underwater acoustic channels, where OFDM symbol duration exceeds channel coherent time. Time-varying channels would introduce inter-carrier interference (ICI), destroy the orthogonality among sub-carriers, and degrade the system performance [4], [5]. The problem gets much more complicated if multiple-input multiple-output (MIMO) structure is adopted, because on each subcarrier of a specific receiver, signals and ICI from all transmitters are mixed up.

Two major problems exist in ICI mitigation in OFDM systems. One is estimation – estimation of the time-varying channel with appropriate model to achieve balance between estimation accuracy and computational complexity, and to avoid overfitting. For example, complex frequency-domain channel estimation methods were used [6], [7], with pilots and null subcarriers. In [8] and [9], compressed sensing has been adopted in TDS-OFDM for long-delay time-varying channel estimation. In MIMO TDS-OFDM systems, PN-Extended and Rotated (PN-ER) sequence is a good choice for MIMO channel estimation [10], [11].

The other problem is equalization – estimating the transmitted symbols from the ICI polluted received signals is usually too complicated for online applications. Thus low-complexity and effective equalization is quite necessary in time-varying channels, especially for MIMO-OFDM systems. This is also the focus of this paper.

Different methods have been proposed to combat ICI in OFDM systems. In [12], perfect channel knowledge is assumed. The performance of matching filter (MF), least-square (LS), minimum mean square error (MMSE) and decision-aided MMSE methods combating ICI are evaluated. In [13], linear ICI-cancellation filters are used to maximize the output signal-to-interference-plus-noise ratio (SINR), with the channel statistics as a requisite. These methods all suffer from huge computational complexity. A number of complexity-reduced ICI mitigation methods are also developed during the years. In [14], a block diagonal channel matrix is used to animate ICI, but the complexity is too high although

the matrix computation scale is reduced. A decision-aided reduced-complexity MMSE equalizer is proposed in [15]. Decision aided ICI cancellation methods are also proposed in [16] and [17] in CP-OFDM.

To directly estimate symbols from the ICI contaminated signal, [18] introduced a low complexity equalization method without matrix inversion for TDS-OFDM. The method is further developed and analyzed in [19] and [20]. Most of these algorithms are designed for single-input single-output (SISO) systems, few were considered for MIMO-OFDM systems. Similar approach in first steps as in [18] is adopted in [21] but it uses Newton's iteration instead for matrix inversion in SISO and MIMO systems. However, the selection of the initial matrix in its Newton method inherently needs a matrix inversion, even though it operates on a block-diagonal matrix.

In this paper, we propose a low-complexity ICI mitigation algorithm in MIMO systems based on similar channel model as in [18]. The method is based on no assumption but linear time-varying (LTV) channel, which is a good approximation when the normalized Doppler frequency is up to 0.2 [21], [22]. It exploits the structure of ICI in MIMO systems and decouples the symbols and the ICIs on each subcarrier. At the same time, it remains low complexity. Simulation shows that the algorithm outperforms the conventional equalizer based on time-invariant channel assumption by about 2 dB when the uncoded bit error rate is  $10^{-3}$ . The proposed method works perfectly when there are more receive units than transmit ones. The methodology implied in the low-complexity MIMO ICI mitigation is to divide the equalization process according to the structure of ICI contribution in linear time-varying channels, and demodulate the symbols independently on each subcarrier.

The remainder of this paper is organized as follows. In Section II, the MIMO TDS-OFDM system based on LTV channel model is described. The MIMO ICI mitigation algorithm is proposed in Section III. In Section IV, the complexity of the algorithm is evaluated. Simulation results are addressed in Section V and Section VI concludes this paper.

**Notation:** Boldface letters denote matrices and vectors. Superscripts  $(\cdot)^T$ ,  $(\cdot)^H$ ,  $(\cdot)^{-1}$ , and  $(\cdot)^\dagger$  denote transpose, conjugate transpose, matrix inversion and Moore-Penrose matrix inversion, respectively.

$\text{Diag}(\mathbf{x})$  is a diagonal matrix with vector  $\mathbf{x}$  on its diagonal,  $\text{diag}(\mathbf{X})$  is the diagonal vector of square matrix  $\mathbf{X}$ , and  $\mathbf{X}(m, n)$  is the  $(m, n)$ -th element of matrix  $\mathbf{X}$ .  $\mathbf{F}_K$  denotes the  $K$ -point discrete Fourier transform (DFT) matrix.

## II. SYSTEM MODEL

In this section, MIMO-OFDM transmission model in linear time-varying channels is introduced. The MIMO TDS-OFDM frame structure is also introduced as one of the possible frame structures that could be applied in our proposed approach for it can easily estimate linear time-varying channels.

### A. MIMO-OFDM in Linear Time-Varying Channels

For MIMO-OFDM, denote the number of transmitters and receivers to be  $M$  and  $N$ , and the OFDM symbol length

to be  $K$ . Denote the  $l$ -th channel tap between the  $m$ -th transmitter and the  $n$ -th receiver at time slot  $t$  by  $h_{l,m,n}^{(t)}$ ,  $l = 0, 1, \dots, L-1$ , where  $L$  is the channel length. Therefore, for linear time-varying channel model in one frame,  $h_{l,m,n}^{(t)} = h_{l,m,n} + \delta_{t-l}\alpha_{l,m,n}$ , where  $h_{l,m,n} = \frac{1}{K} \sum_{t=l}^{l+K-1} h_{l,m,n}^{(t)}$  is the time-invariant part and  $\alpha_{l,m,n}$  is the time-varying factor of its  $l$ -th channel tap.  $\delta_i = \frac{i}{K} - \frac{K-1}{2K}$  indicates the time varying step.

In [18] and [19], the input-output relationship of SISO-OFDM in linear time-varying channels has been introduced. For MIMO-OFDM, by regarding each pair of transmitter  $m$  and receiver  $n$  as a SISO-OFDM link, and by similar approach in [18] and [19], the time domain signal received at the  $n$ -th receiver from the  $m$ -th transmitter could be represented as

$$\mathbf{y}_{m,n} = (\mathbf{H}_{m,n} + \mathbf{A}_{m,n}\mathbf{B})\mathbf{x}_m \quad (1)$$

where  $\mathbf{x}_m$  is the time domain sequence transmitted from the  $m$ -th transmitter,  $\mathbf{H}_{m,n}$  is a  $K \times K$  circulant matrix with the first column to be  $[h_{0,m,n}, h_{1,m,n}, \dots, h_{L-1,m,n}, 0, \dots, 0]^T$ ,  $\mathbf{A}_{m,n}$  is a  $K \times K$  circulant matrix with the first column to be  $[\alpha_{0,m,n}, \alpha_{1,m,n}, \dots, \alpha_{L-1,m,n}, 0, \dots, 0]^T$ ,  $\mathbf{B}$  is a diagonal matrix such that  $\mathbf{B} = \text{Diag}([\delta_0, \delta_1, \dots, \delta_{K-1}]^T)$ .

Convert the signals to frequency domain,

$$\mathbf{Y}_{m,n} = (\mathbf{H}_{m,n} + \mathbf{A}_{m,n}\mathbf{B})\mathbf{X}_m, \quad (2)$$

where  $\mathbf{Y}_{m,n} = \mathbf{F}_K \mathbf{y}_{m,n}$  and  $\mathbf{X}_m = \mathbf{F}_K \mathbf{x}_m$  are the received and transmitted frequency domain symbol vectors.  $\mathbf{H}_{m,n} = \mathbf{F}_K \mathbf{H}_{m,n} \mathbf{F}_K^H = \text{Diag}(\{H_{m,n,k}\}_{k=1}^K)$  and  $\mathbf{A}_{m,n} = \mathbf{F}_K \mathbf{A}_{m,n} \mathbf{F}_K^H = \text{Diag}(\{A_{m,n,k}\}_{k=1}^K)$  are diagonal matrices according to the property of circulant matrix.  $\{H_{m,n,k}\}_{k=1}^K$  and  $\{A_{m,n,k}\}_{k=1}^K$  represent the  $K$ -point DFT of  $[h_{0,m,n}, h_{1,m,n}, \dots, h_{L-1,m,n}]^T$  and  $[\alpha_{0,m,n}, \alpha_{1,m,n}, \dots, \alpha_{L-1,m,n}]^T$ , respectively.  $\mathbf{B} = \mathbf{F}_K \mathbf{B} \mathbf{F}_K^H$  is a precalculated matrix.

The ICI components reside in  $\mathbf{A}_{m,n}$ , and the time invariant components reside in  $\mathbf{H}_{m,n}$ . For SISO-OFDM where  $M = N = 1$ , low complexity ICI compensation in linear time-varying channel model could be achieved by exploiting the frequency domain input-output relationship (2): with both  $\mathbf{H}_{m,n}$  and  $\mathbf{A}_{m,n}$  being diagonal, and with  $\mathbf{B}$  easily calculated by FFT, matrix inversion approximation by power series representation tremendously reduces the complexity in calculating the equalized symbols of  $\mathbf{Y}_{m,n}$  [18], [19]. For MIMO-OFDM, however, the problem gets much more complicated because the signal from one transmitter encounters interference from other transmitters. With the contribution from multiple transmitters, the ICI components could not be directly decoupled as in SISO-OFDM scenarios. Therefore, in order to pursuit new strategies to compensate ICI for MIMO-OFDM, we need to derive the input-output relationship considering all transmitters as follows.

The received signal at the  $n$ -th receiver is the superposition of the received signals from different transmitters, contaminated by noise,

$$\mathbf{Y}_n = \sum_{m=1}^M \mathbf{Y}_{m,n} = \sum_{m=1}^M (\mathbf{H}_{m,n} + \mathbf{A}_{m,n}\mathbf{B})\mathbf{X}_m + \mathbf{V}_n. \quad (3)$$

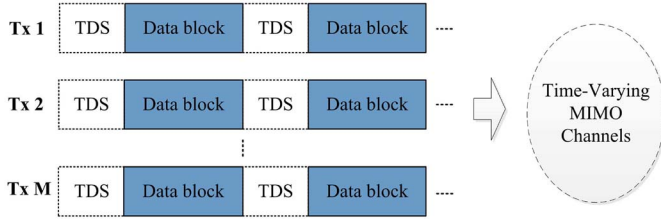


Fig. 1. Frame structure of MIMO TDS-OFDM.

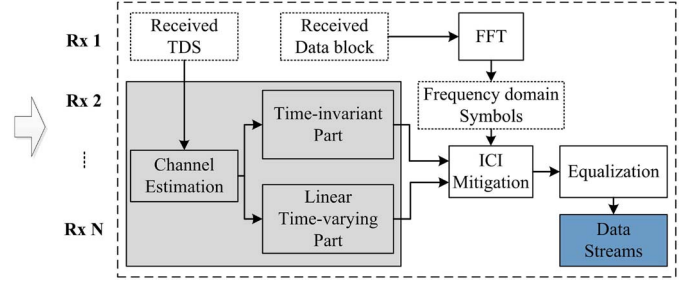


Fig. 2. Receiver side of MIMO TDS-OFDM with ICI mitigation.

$\mathbf{V}_n$  is the frequency domain noise vector at the  $n$ -th receiver. Assume it follows Gaussian distribution  $\mathbf{V}_n \sim \mathcal{N}(\mathbf{0}_{1 \times K}, \delta^2 \mathbf{I}_{K \times K})$ .

Vectorize all received signals, transmitted signals and the frequency domain noise vectors,

$$\mathbf{Y} = [\mathbf{Y}_1^T \mathbf{Y}_2^T \dots \mathbf{Y}_N^T]^T, \quad (4)$$

$$\mathbf{X} = [\mathbf{X}_1^T \mathbf{X}_2^T \dots \mathbf{X}_M^T]^T, \quad (5)$$

$$\mathbf{V} = [\mathbf{V}_1^T \mathbf{V}_2^T \dots \mathbf{V}_N^T]^T, \quad (6)$$

then

$$\mathbf{Y} = \begin{bmatrix} \mathbf{H}'_{1,1} & \mathbf{H}'_{2,1} & \dots & \mathbf{H}'_{M,1} \\ \mathbf{H}'_{1,2} & \mathbf{H}'_{2,2} & \dots & \mathbf{H}'_{M,2} \\ \vdots & \vdots & \ddots & \vdots \\ \mathbf{H}'_{1,N} & \mathbf{H}'_{2,N} & \dots & \mathbf{H}'_{M,N} \end{bmatrix} \mathbf{X} + \mathbf{V} \quad (7)$$

with

$$\mathbf{H}'_{m,n} = \mathbf{H}_{m,n} + \mathbf{A}_{m,n} \mathbf{B}.$$

### B. Introduction of MIMO TDS-OFDM

TDS-OFDM adopts known sequences as the guard interval, serving the purpose of both channel estimation and synchronization [25]. MIMO TDS-OFDM uses pseudo-noise (PN) sequences as the guard interval. In time-varying channels, the channel estimation results from the PN sequences prior to and posteriori to the OFDM data block are put to estimate the channel variation model. In Fig. 1 and Fig. 2, the frame structure and receiver structure of MIMO TDS-OFDM using the proposed ICI mitigation algorithm are illustrated.

### III. PROPOSED ALGORITHM

In the proposed method, firstly rewrite (7) as

$$\begin{aligned} \mathbf{Y} &= (\mathbf{H} + \mathbf{A}\bar{\mathbf{B}})\mathbf{X} + \mathbf{V} = [\mathbf{H} \quad \mathbf{A}] \begin{bmatrix} \mathbf{I} \\ \bar{\mathbf{B}} \end{bmatrix} \mathbf{X} + \mathbf{V} \\ &= [\mathbf{H} \quad \mathbf{A}]\tilde{\mathbf{X}} + \mathbf{V} = [\mathbf{H} \quad \mathbf{A}] \begin{bmatrix} \mathbf{X} \\ \mathbf{X}' \end{bmatrix} + \mathbf{V}, \end{aligned} \quad (8)$$

where

$$\mathbf{H} = \begin{bmatrix} \mathbf{H}_{1,1} & \mathbf{H}_{2,1} & \dots & \mathbf{H}_{M,1} \\ \mathbf{H}_{1,2} & \mathbf{H}_{2,2} & \dots & \mathbf{H}_{M,2} \\ \vdots & \vdots & \ddots & \vdots \\ \mathbf{H}_{1,N} & \mathbf{H}_{2,N} & \dots & \mathbf{H}_{M,N} \end{bmatrix}, \quad (9)$$

$$\mathbf{A} = \begin{bmatrix} \mathbf{A}_{1,1} & \mathbf{A}_{2,1} & \dots & \mathbf{A}_{M,1} \\ \mathbf{A}_{1,2} & \mathbf{A}_{2,2} & \dots & \mathbf{A}_{M,2} \\ \vdots & \vdots & \ddots & \vdots \\ \mathbf{A}_{1,N} & \mathbf{A}_{2,N} & \dots & \mathbf{A}_{M,N} \end{bmatrix}, \quad (10)$$

$$\bar{\mathbf{B}} = \begin{bmatrix} \mathbf{B} & & & \\ & \mathbf{B} & & \\ & & \ddots & \\ & & & \mathbf{B} \end{bmatrix}, \quad (11)$$

and

$$\tilde{\mathbf{X}} = \begin{bmatrix} \mathbf{I} \\ \bar{\mathbf{B}} \end{bmatrix} \mathbf{X} = \begin{bmatrix} \mathbf{X} \\ \bar{\mathbf{B}}\mathbf{X} \end{bmatrix} = \begin{bmatrix} \mathbf{X} \\ \mathbf{X}' \end{bmatrix}. \quad (12)$$

In (12), the original transmitted symbols compose the vector  $\mathbf{X}$ . Then what does the vector  $\mathbf{X}'$  stand for? Actually,  $\mathbf{X}' = \bar{\mathbf{B}}\mathbf{X}$ , and it is multiplied by  $\mathbf{A}$  to construct the ICI. As  $\mathbf{X} = \{X_{n,k}\}_{n=1,k=1}^{N,K} = [\mathbf{X}_1^T, \mathbf{X}_2^T, \dots, \mathbf{X}_N^T]^T$ ,  $\mathbf{X}'$  is similarly formed as  $\mathbf{X}' = \{X'_{n,k}\}_{n=1,k=1}^{N,K} = [\mathbf{X}'_1^T, \mathbf{X}'_2^T, \dots, \mathbf{X}'_N^T]^T$ . In correspondence with  $X_{n,k}$  which denotes the transmitted symbol at the  $k$ -th subcarrier from the  $n$ -th transmitter, the component  $X'_{n,k}$  in  $\mathbf{X}'$  stands for the interference at the  $k$ -th subcarrier 'from' the  $n$ -th transmitter. It's noted that the interference among different subcarriers is handled by  $\bar{\mathbf{B}}$ , so  $X'_{n,k}$  is the interference only on subcarrier  $k$ . Therefore, Matrix  $\mathbf{H}$  represents the channel time-invariant part and describes the signal transfer without interference. Matrix  $\mathbf{A}$  represents the channel time-varying part and describes the interference transfer itself.

Regard the system transfer function in (8) as a  $2M$ -transmitter  $N$ -receiver MIMO-OFDM with  $K$  subcarriers. As mentioned above, there is no intercarrier interference any more in the equivalent system, therefore the equalizer can be parallelized on each subcarrier.

For subcarrier  $k$ ,

$$\bar{\mathbf{Y}}_k = [Y_{1,k} Y_{2,k} \dots Y_{N,k}]^T, \quad (13)$$

$$\tilde{\mathbf{X}}_k = [X_{1,k} X_{2,k} \dots X_{M,k}, X'_{1,k} X'_{2,k} \dots X'_{M,k}]^T, \quad (14)$$

$$\bar{\mathbf{H}}_k = \begin{bmatrix} H_{1,1,k} & H_{2,1,k} & \dots & H_{M,1,k} \\ H_{1,2,k} & H_{2,2,k} & \dots & H_{M,2,k} \\ \vdots & \vdots & \ddots & \vdots \\ H_{1,N,k} & H_{2,N,k} & \dots & H_{M,N,k} \end{bmatrix}, \quad (15)$$

$$\bar{\mathbf{A}}_k = \begin{bmatrix} A_{1,1,k} & A_{2,1,k} & \dots & A_{M,1,k} \\ A_{1,2,k} & A_{2,2,k} & \dots & A_{M,2,k} \\ \vdots & \vdots & \ddots & \vdots \\ A_{1,N,k} & A_{2,N,k} & \dots & A_{M,N,k} \end{bmatrix}, \quad (16)$$

TABLE I  
COMPLEXITY COMPARISON OF DIFFERENT EQUALIZERS

Method	Complexity (in number of complex multiplications)
LMMSE in LTI <sup>1</sup>	$O(K(N^3 + MN^2 + MN + N \log(K)))$
Proposed in LTV <sup>2</sup>	$O(K(N^3 + 2MN^2 + 2MN + 2M^2 + N \log(K)))$
Original in LTV <sup>3</sup>	$O(K^3(N^3 + MN^2 + MN) + NK \log(K))$

<sup>1</sup> LMMSE equalizer under the assumption of linear time-invariant channels.

<sup>2</sup> Proposed equalization with ICI mitigation in linear time-varying channels.

<sup>3</sup> Direct manipulation of (8) in linear time-varying channels.

and

$$\bar{\mathbf{Y}}_k = [\bar{\mathbf{H}}_k \quad \bar{\mathbf{A}}_k] \tilde{\mathbf{X}}_k + \bar{\mathbf{V}}_k. \quad (17)$$

This is a standard flat-fading MIMO system transfer expression with the transmitted symbol vector  $\tilde{\mathbf{X}}_k$  and received vector  $\bar{\mathbf{Y}}_k$ . Therefore, traditional OFDM equalizer with  $2M$  transmitters and  $N$  receivers could be used to equalize the transmitted symbols on subcarrier  $k$  [23], [24].

When a linear MMSE (LMMSE) equalizer is used,

$$\tilde{\mathbf{X}}_k \approx \mathbf{C}_{\tilde{\mathbf{X}}_k} \begin{bmatrix} \bar{\mathbf{H}}_k^H \\ \bar{\mathbf{A}}_k^H \end{bmatrix} \left( \begin{bmatrix} \bar{\mathbf{H}}_k & \bar{\mathbf{A}}_k \end{bmatrix} \mathbf{C}_{\tilde{\mathbf{X}}_k} \begin{bmatrix} \bar{\mathbf{H}}_k^H \\ \bar{\mathbf{A}}_k^H \end{bmatrix} + \delta \mathbf{I} \right)^{-1} \bar{\mathbf{Y}}_k. \quad (18)$$

The vector  $\tilde{\mathbf{X}}$  contains the estimation of the transmitted symbols. To achieve better estimation performance,  $\mathbf{X}$  is estimated as

$$\begin{aligned} \hat{\mathbf{X}} &= \mathbf{E} \tilde{\mathbf{X}} = \mathbf{C}_{\tilde{\mathbf{X}}\tilde{\mathbf{X}}} \mathbf{C}_{\tilde{\mathbf{X}}\tilde{\mathbf{X}}}^{-1} \tilde{\mathbf{X}} \\ &= [\mathbf{I} \quad \bar{\mathbf{B}}^H] \begin{bmatrix} \mathbf{I} & \bar{\mathbf{B}}^H \\ \bar{\mathbf{B}} & \bar{\mathbf{B}}\bar{\mathbf{B}}^H \end{bmatrix}^{-1} \tilde{\mathbf{X}}. \end{aligned} \quad (19)$$

with the matrix

$$\begin{aligned} \mathbf{E} &= \mathbf{C}_{\tilde{\mathbf{X}}\tilde{\mathbf{X}}} \mathbf{C}_{\tilde{\mathbf{X}}\tilde{\mathbf{X}}}^{-1} \\ &= [\mathbf{I} \quad \bar{\mathbf{B}}^H] \begin{bmatrix} \mathbf{I} & \bar{\mathbf{B}}^H \\ \bar{\mathbf{B}} & \bar{\mathbf{B}}\bar{\mathbf{B}}^H \end{bmatrix}^{-1}. \end{aligned} \quad (20)$$

Although inversion of a large matrix is involved in (19), the calculation of matrix  $\mathbf{E}$  is determined only by  $M$ ,  $N$  and  $K$ , thus it's irrelevant to channel realization. Therefore  $\mathbf{E}$  is a precalculated matrix and acts like a predesigned linear filter, the complexity is limited to filtering itself.  $\mathbf{C}_{\tilde{\mathbf{X}}_k}$  in (18) is the covariance matrix of the transmitted symbol vector. The inversion of the  $\mathbf{C}_{\tilde{\mathbf{X}}_k}$  can also be pre-calculated because the matrix is a  $2M \times 2M$  submatrix composing of the elements at the  $k$ -th,  $K+k$ -th, ... and  $(2M-1)K+k$ -th rows and columns of the matrix  $\mathbf{C}_{\tilde{\mathbf{X}}\tilde{\mathbf{X}}}$ .

In comparison, the conventional LMMSE equalizer in MIMO-OFDM also works subcarrier by subcarrier. The only difference is that the subsystem transfer function in each subcarrier does not contain the time varying matrix  $\bar{\mathbf{A}}_k$ ,

$$\bar{\mathbf{Y}}_k = \bar{\mathbf{H}}_k \tilde{\mathbf{X}}_k + \bar{\mathbf{V}}_k. \quad (21)$$

So the demodulation in LTI channels is

$$\tilde{\mathbf{X}}_k \approx \mathbf{C}_{\tilde{\mathbf{X}}_k} \bar{\mathbf{H}}_k^H (\bar{\mathbf{H}}_k \mathbf{C}_{\tilde{\mathbf{X}}_k} \bar{\mathbf{H}}_k^H + \delta \mathbf{I})^{-1} \bar{\mathbf{Y}}_k. \quad (22)$$

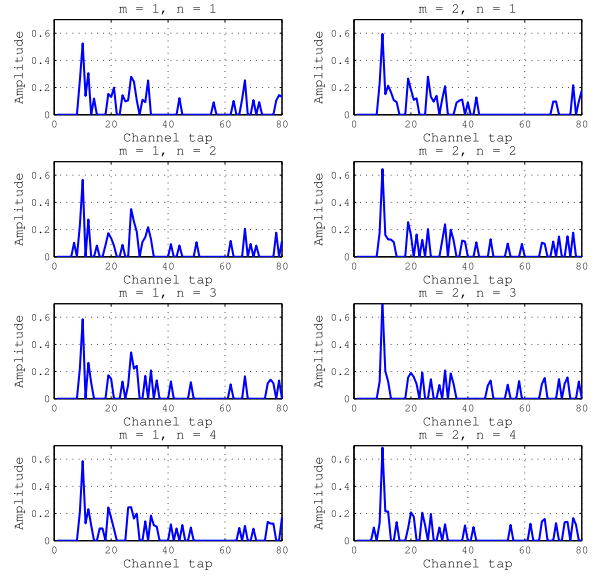


Fig. 3. MIMO channel impulse responses when  $M = 2$  and  $N = 4$ .

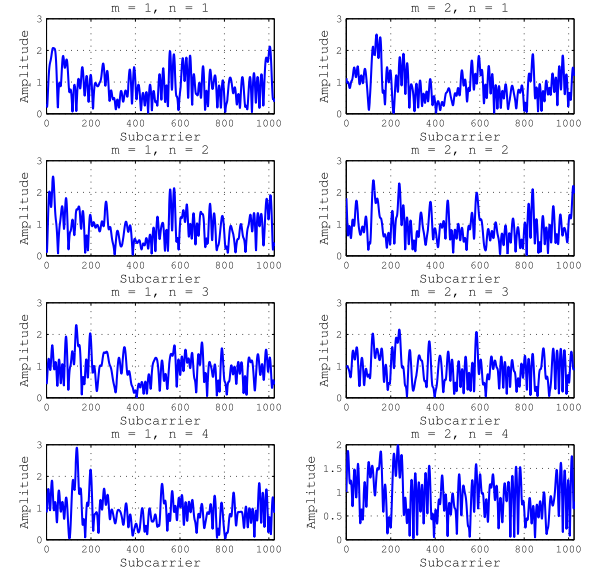
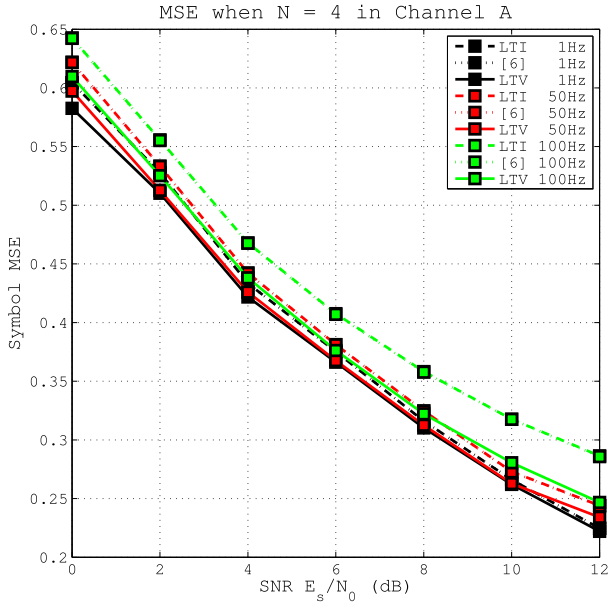
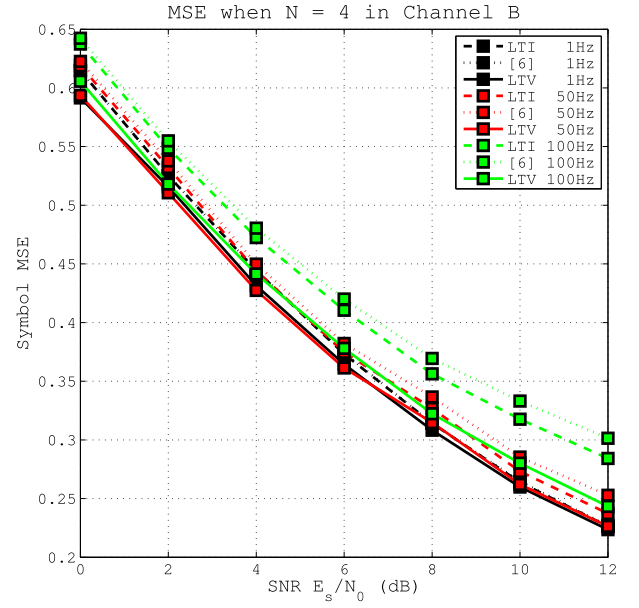
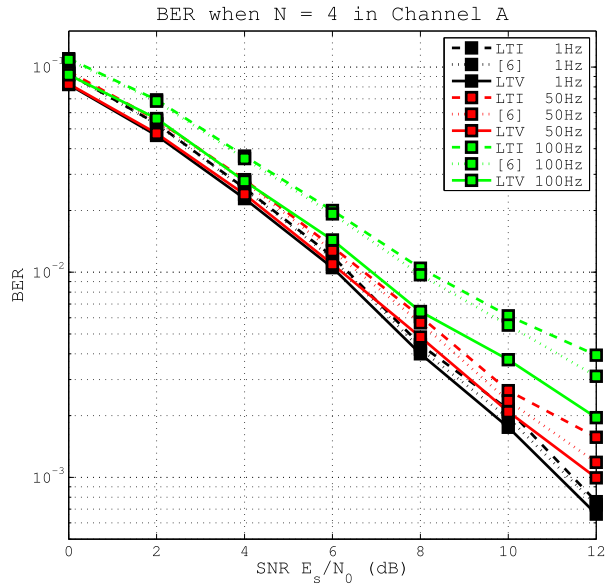
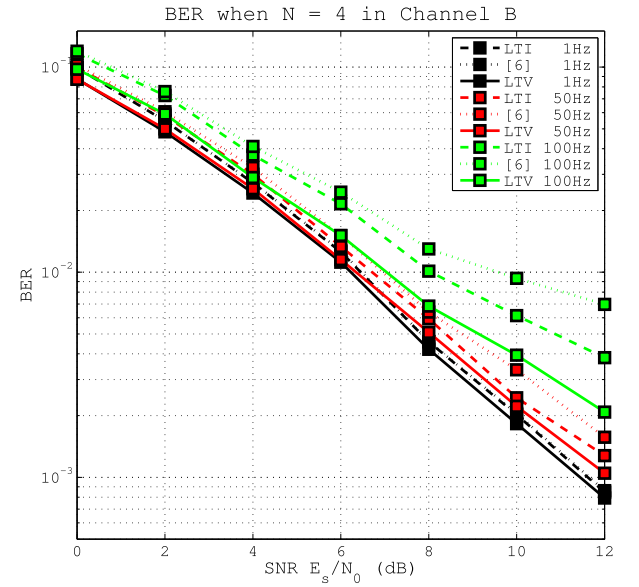


Fig. 4. MIMO channel frequency domain response when  $M = 2$  and  $N = 4$ .

#### IV. COMPLEXITY ANALYSIS

In this section, the complexity of the proposed equalization algorithm under the assumption of linear time-varying channels and the conventional LMMSE equalizer under the assumption of time invariant channels is evaluated and compared.

For equalization under LTI channel assumption, most of the computations occurs when doing matrix multiplication for each subcarrier as in (22). The matrix to be inverted is a  $N$ -by- $N$  matrix, therefore the inversion complexity is  $O(N^3)$  complex number multiplications. With the complexity of matrix multiplication ( $MN^2$ ) and matrix-vector multiplication ( $MN$ ) added up, the complexity is  $O(N^3 + MN^2 + MN)$  for the data processing on each subcarrier. If the complexity of FFT and IFFT at each receiver is counted as  $O(K \log(K))$ ,

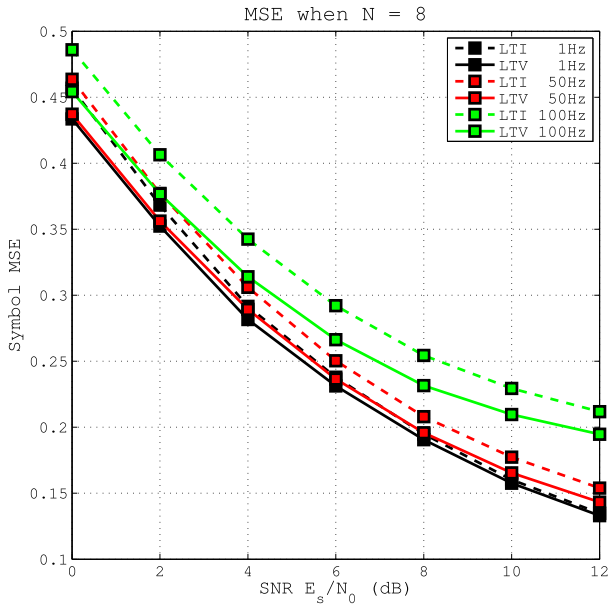
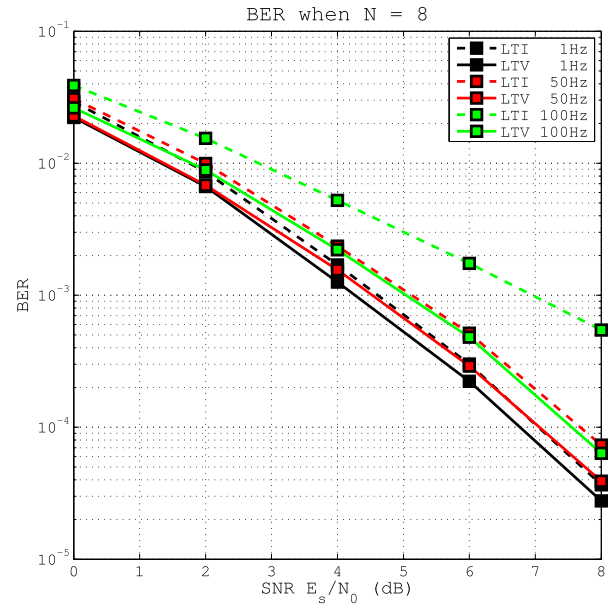
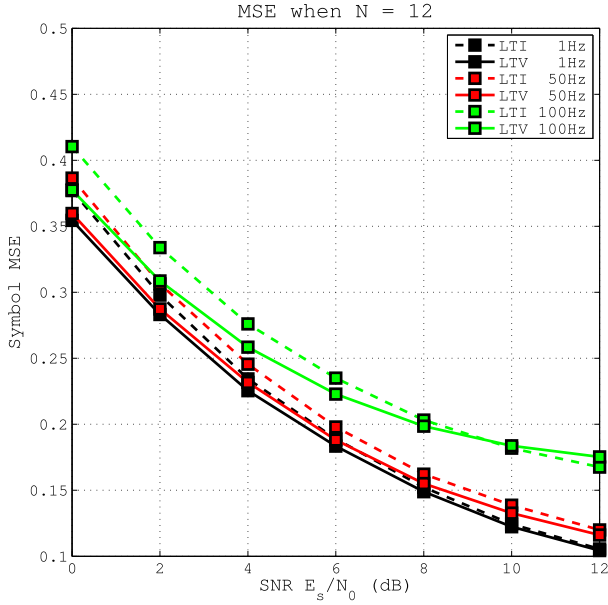
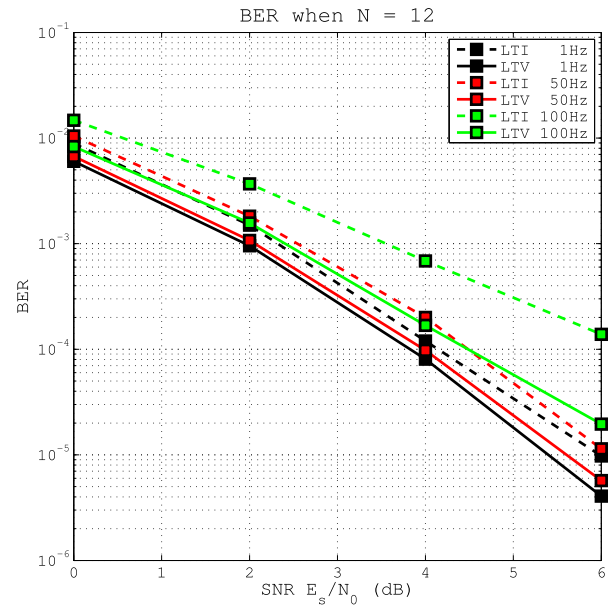
Fig. 5. Equalization MSE of QPSK when  $N = 4$  in Channel A.Fig. 7. Equalization MSE of QPSK when  $N = 4$  in Channel B.Fig. 6. Equalization BER of QPSK when  $N = 4$  in Channel A.Fig. 8. Equalization BER of QPSK when  $N = 4$  in Channel B.

then the total complexity of the equalizer in LTI channel is  $O(K(N^3 + MN^2 + MN + N \log(K)))$ .

For the proposed equalizer with ICI mitigation, the complexity of matrix inversion is also  $O(N^3)$  for each subcarrier. Multiplications of matrices and vector contribute  $O(2MN^2 + 2MN)$  complex number multiplications. The additional linear filtering in (19) contributes  $O(KM^2)$  in total. Therefore, considering FFT, IFFT and data processing on all subcarriers, the complexity of the proposed method is  $O(K(N^3 + 2MN^2 + 2MN + 2M^2 + N \log(K)))$ .

For both of the algorithms, the complexity is linear to the number of subcarriers, and cubic to the number of receivers, when the numbers of transmitters and receivers are on the same order. So the proposed algorithm has remained fairly

low complexity even compared with the equalizer in LTI channels. It is noted that if the explicit ICI decomposition and mitigation were not conducted as in the proposed algorithm, we need to make matrix inversion on the scale of the big matrix  $\mathbf{H} + \mathbf{A}\mathbf{B}$  in (8) directly. In this condition, the computation of  $\mathbf{A}\mathbf{B}$  have  $O(K^3MN)$  complex multiplications as  $\mathbf{B}$  is a block diagonal matrix. FFTs and matrix inversion contribute  $O((KN)^3 + K^3MN^2 + NK \log(K))$ . So the total computational complexity is  $O(K^3(N^3 + MN^2 + MN) + NK \log(K))$ , which is far more complex number multiplications than that is needed in the proposed one. The computation complexity of the three algorithms is demonstrated in Table I. It has shown that the proposed algorithm has successfully reduced the complexity of the original problem to a great extent.

Fig. 9. Equalization MSE performance of QPSK when  $N = 8$ .Fig. 11. Equalization BER performance of QPSK when  $N = 8$ .Fig. 10. Equalization MSE performance of QPSK when  $N = 12$ .Fig. 12. Equalization BER performance of QPSK when  $N = 12$ .

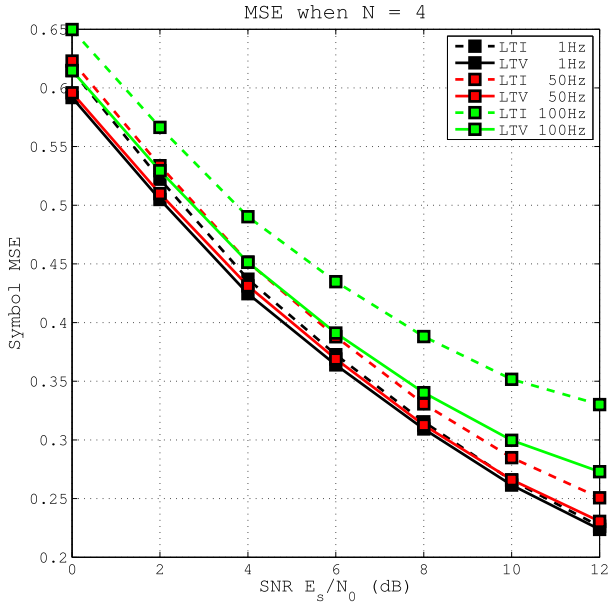
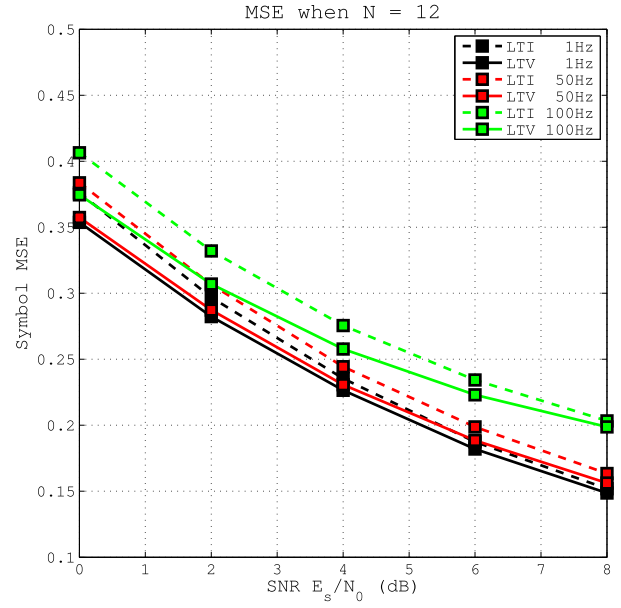
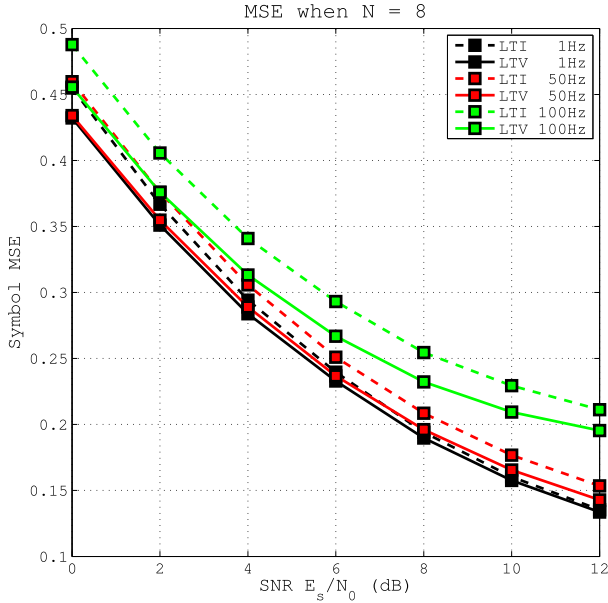
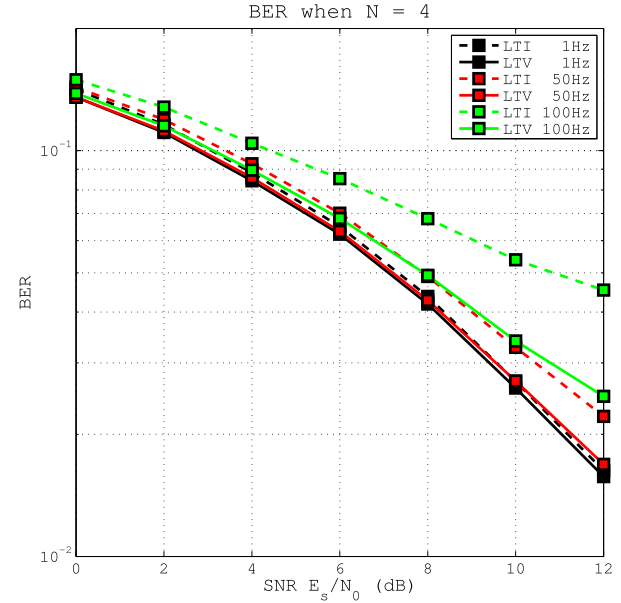
## V. SIMULATION RESULT

Simulations are conducted to evaluate the performance of the proposed algorithm. The conventional equalizer under the assumption of time invariant channel is also tested for comparison.

The number of transmitters is chosen to be 2, and the number of receivers is 4, 8, and 12. The system takes MIMO TDS-OFDM structure with PN-Extended and Rotated (PN-ER) [10], [11] as the time domain sequences to conveniently estimate the MIMO channels. The bandwidth is 1 MHz and the system has  $K = 1024$  subcarriers, so each subcarrier bears about 1 kHz of bandwidth. The information bits are independently and uncodedly QPSK/16QAM modulated on each transmitter. The simulation takes MIMO

channel delay profiles and changes the Doppler frequency of the Rayleigh fading channels to test the performance of the proposed algorithm. The maximum Doppler shift in the simulation is 100 Hz, or equivalently a Doppler factor of 0.1. As shown in Fig. 3 and Fig. 4, the channel suffers from long multipath delay and is highly frequency selective.

As a benchmark, the conventional equalizer under the assumption of linear time-invariant channel is identified by “LTI”. Another algorithm to be compared is the ICI mitigation method introduced in [6], where the time-varying channel in MIMO-OFDM is modeled to have a common frequency offset on each receiver relative to all transmitters. In [6], the frequency offset is estimated by frequency domain pilots and

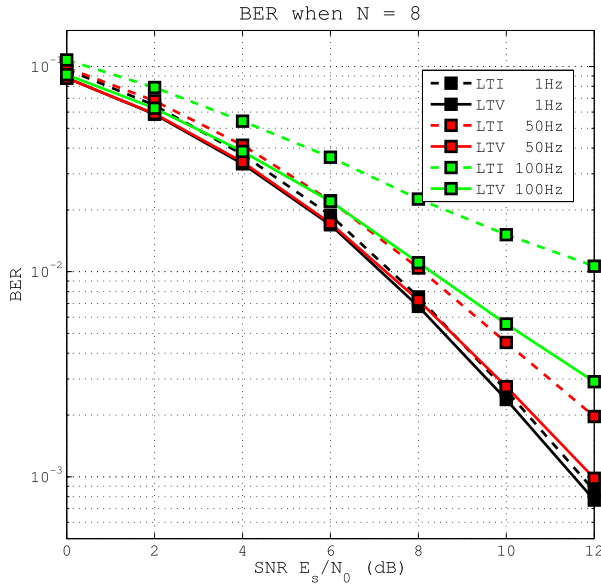
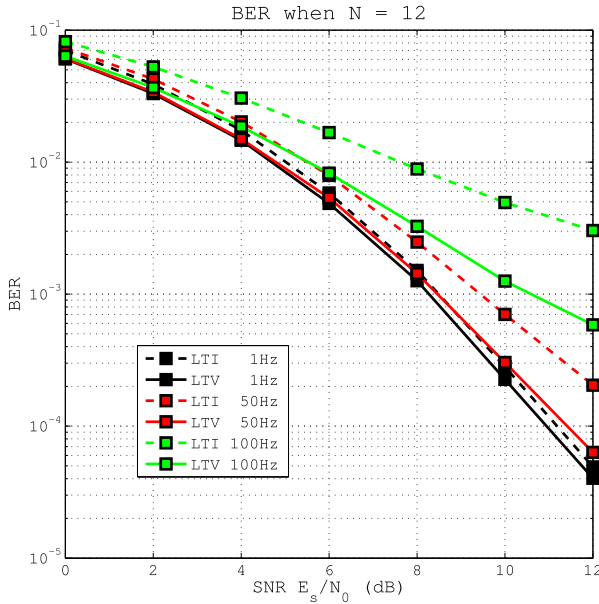
Fig. 13. Equalization MSE performance of 16QAM when  $N = 4$ .Fig. 15. Equalization MSE performance of 16QAM when  $N = 12$ .Fig. 14. Equalization MSE performance of 16QAM when  $N = 8$ .Fig. 16. Equalization BER performance of 16QAM when  $N = 4$ .

by minimizing the energy on the null subcarriers, but in our TDS-OFDM model, we estimate the offset by the time-domain sequences. Our proposed algorithm is identified by “LTV”. It’s noted that the complexity of direct manipulation that deal with (8) is too high to be computational affordable (about  $10^6$  times higher than the proposed algorithm when  $K = 1024$ ), therefore its performance is not provided in the simulation.

To demonstrate the performance of the proposed algorithm, we first compare the three algorithms in the presence of two different channels. The first channel (“Channel A”) is the channel with the Doppler spectrum following a Gaussian distribution. The centered Doppler frequency is  $0.9f_D$ , and the sigma of the Gaussian distribution is  $0.001f_D$ , where  $f_D$  is the maximum Doppler shift. Therefore, this channel is a channel

that has nearly a dominant Doppler shift. For the other channel (“Channel B”), the Doppler spread of all paths follows Jakes Doppler spectrum with maximum Doppler shift  $f_D$ . So Channel B has more sophisticated time-varying feature than Channel A.

In Fig. 5 and Fig. 6, the MSE and uncoded bit error rate (BER) performance of the three algorithms is compared in Channel A with QPSK modulation, when  $f_D = 1$  Hz, 50 Hz and 100 Hz. In Fig. 7 and Fig. 8, their performance is compared in Channel B with QPSK modulation. In Channel A, where a common dominant Doppler shift has the most impact on the time-varying channels, the method in [6] has about 0.3 dB symbol signal to noise ratio (SNR) advantage over the “LTI” equalizer when BER is between  $10^{-3}$  and  $10^{-2}$ ,

Fig. 17. Equalization BER performance of 16QAM when  $N = 8$ .Fig. 18. Equalization BER performance of 16QAM when  $N = 12$ .

because Channel A almost obeys its channel fading assumption. However, in Channel B, “LTI” performs better than the algorithm in [6] because different channel paths may have different time-varying profiles thus violate the assumption of the algorithm in [6]. In both Channel A and Channel B, the proposed algorithm has shown the best MSE and BER performance among the three.

In the following comparison, Channel B is used because it has a more generalized fading model. The proposed algorithm is compared with the conventional algorithm under assumption. The algorithm of [6] is not included in the comparison because it does not perform well in Channel B.

The MSE performance with different Doppler frequencies with  $N = 8, 12$  is shown in Fig. 9 and Fig. 10 for QPSK

modulation and with  $N = 4, 8, 12$  in Fig. 13, Fig. 14 and Fig. 15 for 16QAM modulation, respectively.

From these figures, we could see that the MSE of both algorithms grows when the maximum Doppler shift increases, which reflects more severe impact of intercarrier interference increased with the maximum Doppler shift. The MSE gets smaller when more receivers are used, which is a result of more diversity gain with more receiving units. At the same time, when  $f_D = 1$  Hz, 50 Hz and 100 Hz, the proposed algorithm always has a smaller MSE than the conventional equalizer.

The BER performance is demonstrated by Fig. 11 and Fig. 12 for QPSK and by Fig. 16, Fig. 17 and Fig. 18 for 16QAM. The proposed algorithm also outperforms the LTI equalizer when the Doppler frequency is 1 Hz, 50 Hz and 100 Hz. The SNR gain when the BER is around  $10^{-3}$  gets larger when the Doppler frequency increases: 0.2 dB when  $f_D = 1$  Hz, 0.6 dB when  $f_D = 50$  Hz and about 2 dB when  $f_D = 100$  Hz.

Both MSE and BER performance has shown that the proposed algorithm has an obvious advantage over the conventional LTI equalizer. According to our computational complexity analysis, the performance promotion is at the expense with only a small extra computational complexity. Compared with the algorithm in [6], the proposed method is feasible to more sophisticated channel fading conditions, allowing independent time-varying profiles for different channel paths and for different transmitter-receiver pairs.

## VI. CONCLUSION

In this paper, a low complexity ICI mitigation algorithm in MIMO-OFDM is proposed. The algorithm exploits the ICI contribution structure in linear time varying channels and maintains low complexity. Simulations have shown that the proposed method outperforms the conventional equalization under LTI assumption by up to 2 dB SNR advantage when the relative Doppler factor is 0.1.

The algorithm is an MIMO extension from the SISO algorithms proposed in [18]–[20]. These algorithms all make use of linear time variation model to achieve low complexity ICI compensation in OFDM systems. Future work on related or extended algorithms based on this work is possible, such as equalization with iterative interference cancellation and turbo equalization with soft information calculation.

## REFERENCES

- [1] B. Muquet, Z. Wang, G. B. Giannakis, M. De Courville, and P. Duhamel, “Cyclic prefixing or zero padding for wireless multicarrier transmissions?” *IEEE Trans. Commun.*, vol. 50, no. 12, pp. 2136–2148, Dec. 2002.
- [2] L. Hanzo, M. Munster, B. J. Choi, and T. Keller, *OFDM and MC-CDMA for Broadband Multi-User Communications, WLANs, and Broadcasting*. Chichester, U.K.: Wiley, 2003.
- [3] L. Dai, Z. Wang, and Z. Yang, “Next-generation digital television terrestrial broadcasting systems: Key technologies and research trends,” *IEEE Commun. Mag.*, vol. 50, no. 6, pp. 150–158, Jun. 2012.
- [4] J. Armstrong, “Analysis of new and existing methods of reducing inter-carrier interference due to carrier frequency offset in OFDM,” *IEEE Trans. Commun.*, vol. 47, no. 3, pp. 365–369, Mar. 1999.

- [5] H.-C. Wu, "Analysis and characterization of intercarrier and interblock interferences for wireless mobile OFDM systems," *IEEE Trans. Broadcast.*, vol. 52, no. 2, pp. 203–210, Jun. 2006.
- [6] B. Li *et al.*, "MIMO-OFDM for high-rate underwater acoustic communications," *IEEE J. Ocean. Eng.*, vol. 34, no. 4, pp. 634–644, Oct. 2009.
- [7] J. Huang, S. Zhou, and Z. Wang, "Performance results of two iterative receivers for distributed MIMO OFDM with large Doppler deviations," *IEEE J. Ocean. Eng.*, vol. 38, no. 2, pp. 347–357, Apr. 2013.
- [8] L. Dai, Z. Wang, J. Wang, and Z. Yang, "Joint time-frequency channel estimation for time domain synchronous OFDM systems," *IEEE Trans. Broadcast.*, vol. 59, no. 1, pp. 168–173, Mar. 2013.
- [9] W. Ding, F. Yang, C. Pan, L. Dai, and J. Song, "Compressive sensing based channel estimation for OFDM systems under long delay channels," *IEEE Trans. Broadcast.*, vol. 60, no. 2, pp. 313–321, Jun. 2014.
- [10] D. Du, J. Wang, K. Gong, and J. Song, "A transmit diversity scheme for TDS-OFDM system," *IEEE Trans. Broadcast.*, vol. 54, no. 3, pp. 482–488, Sep. 2008.
- [11] D. Du, J. Wang, J. Wang, and K. Gong, "Orthogonal sequences design and application for multiple access of TDS-OFDM system," in *Proc. Cross Strait Tri-Region. Radio Sci. Wireless Technol. Conf.*, Tianjin, China, 2009, pp. 1–5.
- [12] Y.-S. Choi, P. J. Volts, and F. A. Cassara, "On channel estimation and detection for multicarrier signals in fast and selective Rayleigh fading channels," *IEEE Trans. Commun.*, vol. 49, no. 8, pp. 1375–1387, Aug. 2001.
- [13] A. Stamoulis, S. N. Diggavi, and N. Al-Dhahir, "Inter-carrier interference in MIMO OFDM," *IEEE Trans. Signal Process.*, vol. 50, no. 10, pp. 2451–2464, Oct. 2002.
- [14] W. G. Jeon, K. H. Chang, and Y. S. Cho, "An equalization technique for orthogonal frequency-division multiplexing systems in time-variant multipath channels," *IEEE Trans. Commun.*, vol. 47, no. 1, pp. 27–32, Jan. 1999.
- [15] X. Cai and G. B. Giannakis, "Bounding performance and suppressing intercarrier interference in wireless mobile OFDM," *IEEE Trans. Commun.*, vol. 51, no. 12, pp. 2047–2056, Dec. 2003.
- [16] S. Chen and C. Zhu, "ICI and ISI analysis and mitigation for OFDM systems with insufficient cyclic prefix in time-varying channels," *IEEE Trans. Consum. Electron.*, vol. 50, no. 1, pp. 78–83, Feb. 2004.
- [17] S. Husen and S. Baggen, "Simple Doppler compensation for DVBT," in *Proc. OFDM Workshop*, Dresden, Germany, Jun. 2004, pp. 67–71.
- [18] J. Fu, C.-Y. Pan, Z.-X. Yang, and L. Yang, "Low-complexity equalization for TDS-OFDM systems over doubly selective channels," *IEEE Trans. Broadcast.*, vol. 51, no. 3, pp. 401–407, Sep. 2005.
- [19] J. Hao, J. Wang, and Y. Wu, "A new equalizer in doubly-selective channels for TDS-OFDM," *IEEE Trans. Broadcast.*, vol. 61, no. 1, pp. 91–97, Mar. 2015.
- [20] S. Huang, J. Wang, Z. An, J. Wang, and J. Song, "Iterative MMSE-DFE and error transfer for OFDM in doubly selective channels," *IEEE Trans. Broadcast.*, vol. 61, no. 3, pp. 541–547, Sep. 2015.
- [21] C. Y. Hsu and W. R. Wu, "Low-complexity ICI mitigation methods for high-mobility SISO/MIMO-OFDM systems," *IEEE Trans. Veh. Technol.*, vol. 58, no. 6, pp. 2755–2768, Jul. 2009.
- [22] Y. Mostofi and D. C. Cox, "ICI mitigation for pilot-aided OFDM mobile systems," *IEEE Trans. Wireless Commun.*, vol. 4, no. 2, pp. 765–774, Mar. 2005.
- [23] G. L. Stuber *et al.*, "Broadband MIMO-OFDM wireless communications," *Proc. IEEE*, vol. 92, no. 2, pp. 271–294, Feb. 2004.
- [24] N. S. Randhawa, S. Sharma, and R. K. Dubey, "A survey of equalization techniques for an effective equalizer design in MIMO-OFDM systems," in *Proc. Int. Conf. Circuit Power Comput. Technol. (ICCPCT)*, Nagercoil, India, Mar. 2015, pp. 1–5.
- [25] J. Fu, J. Wang, J. Song, C. Y. Pan, and Z. X. Yang, "A simplified equalization method for dual PN-sequence padding TDS-OFDM systems," *IEEE Trans. Broadcast.*, vol. 54, no. 4, pp. 825–830, Dec. 2008.

**Jinxing Hao**, photograph and biography not available at the time of publication.

**Jintao Wang**, photograph and biography not available at the time of publication.

**Changyong Pan**, photograph and biography not available at the time of publication.